Assessing Water Quality of the Chesapeake Bay by the Impact of Sea Level Rise and Warming

P. Wang[1], L. Linker[2], H. Wang[3], G. Bhatt[4], G. Yactayo[5], K. Hinson[5], and R. Tian[7]

[1] Senior Research Scientist, Virginia Institute Marine Science, Gloucester P, VA, USA
[2] Modeling Coord. USEPA Chesapeake Bay Program Office, Annapolis, MD, USA
[3] Professor, Virginia Institute of Marine Science, Gloucester Point, VA, USA
[4] Research Associate, Penn State University, University Park, PA, USA
[5] Environmental Engineer, Maryland Dept of Environment, Baltimore, MD, USA
[6] Staffer, Chesapeake Research Consortium, Edgewater, MD, USA
[7] Research Associate, Univ of Maryland Center Envir. Sc, Cambridge, MD, USA

Corresponding author: P. Wang, email: pwang@chesapeakebay.net

Abstract. The influence of sea level rise and warming on circulation and water quality of the Chesapeake Bay under projected climate conditions in 2050 were estimated by computer simulation. Four estuarine circulation scenarios in the estuary were run using the same watershed load in 1991-2000 period. They are, 1) the Base Scenario, which represents the current climate condition, 2) a Sea Level Rise Scenario, 3) a Warming Scenario, and 4) a combined Sea Level Rise and Warming Scenario. With a 1.5-1.9^{o}C increase in monthly air temperatures in the Warming Scenario, water temperature in the Bay is estimated to increase by 0.8-1^{o}C. Summer average anoxic volume is estimated to increase 1.4 percent compared to the Base Scenario, because of an increase in algal blooms in the spring and summer, promotion of oxygen consumptive processes, and an increase of stratification. However, a 0.5-meter Sea Level Rise Scenario results in a 12 percent reduction of anoxic volume. This is mainly due to increased estuarine circulation that promotes oxygen-rich sea water intrusion in lower layers. The combined Sea Level Rise and Warming Scenario results in a 10.8 percent reduction of anoxic volume. Global warming increases precipitation and consequently increases nutrient loads from the watershed by approximately 5-7 percent. A scenario that used a 10% increase in watershed loads and current estuarine circulation patterns yielded a 19 percent increase in summer anoxic volume, while a scenario that used a 10% increase in watershed loads and modified estuarine circulation patterns by the aforementioned sea level rise and warming yielded a 6 percent increase in summer anoxic volume. Impacts on phytoplankton, sediments, and water clarity were also analysed.

1. Introduction

To protect the water quality and ecosystems of the Chesapeake Bay a TMDL (total maximum daily load) policy was enacted by the USEPA in December of 2010 [1]. A suite of computer models including the Watershed Model (WSM), estuarine Water Quality and Sediment Transport Model (WQSTM) and ancillary living resource models were used in the development of the 2010 TMDL to establish nutrient and sediment reduction targets to achieve the Chesapeake water quality standards of dissolved oxygen (DO), chlorophyll-*a*, and water clarity [2]. The 2010 TMDL documentation [1] and the 2009 Executive Order [3] also called for an assessment of the impacts of changing climate on Chesapeake Bay water

quality and living resources. The assessment will include projected changes in land use, precipitation, air temperature, water temperature, sea level rise, wetland loss, and water quality in the tidal Bay for 2025 and 2050. The climate change analysis will use the same methodology as that employed in the Chesapeake 2010 TMDL assessment, which applies the WQSTM estuarine model to estimate the influence exerted upon Chesapeake Bay circulation and water quality due to changed climate conditions. This study only involves the impact on water quality due to sea level rise and temperature change, as well as changes in watershed loads due to altered precipitation and temperature in a projected 2050 climate condition.

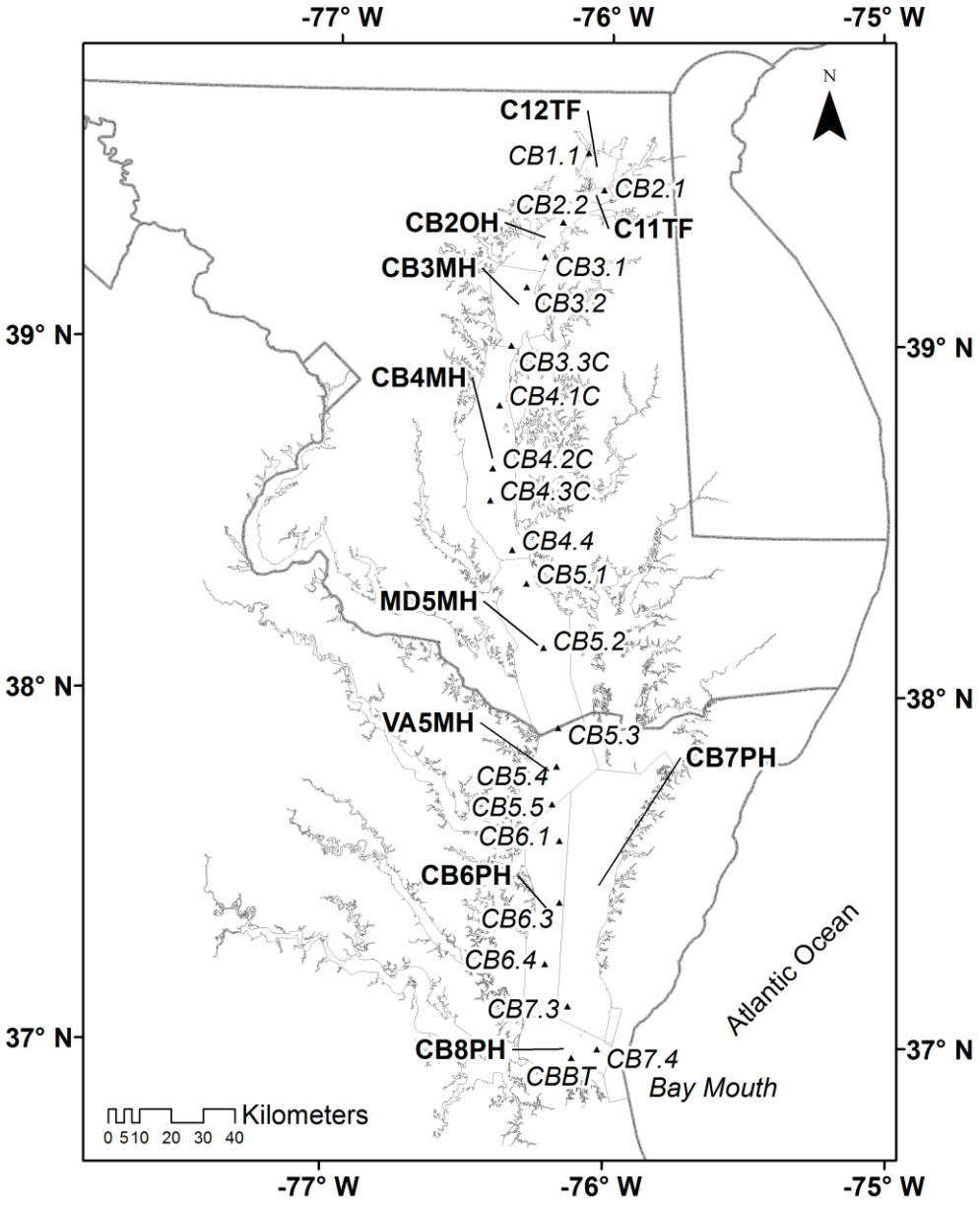

Figure 1. The Chesapeake Bay estuary, its mainstem CB segments, and key monitoring stations along the main channel.

Climate conditions in 2050 have been estimated by various researchers [4-7]. Average air temperatures in 2050 will be higher than the current condition due to global warming (GW), and are estimated to increase by 1.5-2^{o}C [7,8]. According to a linear regression of observed water elevations at the Chesapeake Bay Bridge Tunnel station (CBBT) near the Bay mouth (Fig. 1), sea level rise has occurred at a rate of 0.63 cm/year over the past 30 years [9]. Under a continuation of this trend, local sea level is expected to rise approximately 32 cm between 2000 and 2050. However, considering the acceleration of sea level rise in later years [5], this estimate may increase to 40-50 cm by 2050. This value is consistent with an estimate produced by Parris et al. [5] and Boesch et al. [10]. Associated with historical sea level observations in the Chesapeake Bay, Boesch et al.[10] estimated sea level rise in 2050 (from 2000) to reach about 0.3-0.7 m, with a most likely estimate of 0.4 m. Considering 1995 as the midpoint of the 1991-2000 hydrology used to establish the Chesapeake TMDL, this work uses an estimated 0.5 m sea level rise for 2050 that is consistent with recommendations put forth by the Chesapeake Scientific and Technology Advisory Committee [11].

Sea level rise (SLR) increases salt intrusion into the Bay. Associated with the sea level rise in the past 30 years, the observed salinity in both surface water and bottom water at the Bay mouth increased by about 4 ppt. This is consistent with model simulations completed by Hilton et al. [12]. Hong and Shen [13] simulated salinity in the Chesapeake Bay estuary under a 0.5 meter sea level rise for years 2001 and 2003, and produced similar results [13]. The proper setting of the ocean boundary salinity is an important consideration in this type of model simulation. The assumption of a 0.5 meter sea level rise in this work enables the utilization of Hong and Shen's [13] estimated salinity boundary condition, and the ability to compare simulations [13].

Summer hypoxia/anoxia and its resultant cascade of biogeochemical and ecological effects is a key threat to the Bay's living resources. Hypoxic and anoxic waters are located at regions of stratified deep water. The existence of stratification prevents exchange of DO between the saltier, denser lower layer and the fresher, less dense upper layer and acts to preserve hypoxic conditions in deep waters. The pycnocline, with abrupt changes in density, separates waters in the upper and lower layers. In the 2010 Chesapeake Bay TMDL for DO compliance, DO standards were set for three depth-categories of designated-use, i.e., *Open Water* (OW), *Deep Water* (DW) and *Deep Channel* (DC), individually. The *Open Water* and *Deep Water* designated-uses are separated by the upper boundary of the pycnocline, and the Deep Channel designated-use is below the lower boundary of the pycnocline. Of particular concern is DO attainment in *Deep Water* and *Deep Channel* designated-uses. Nutrient and sediment loads from the watershed and subsequent Bay water quality responses were assessed for the TMDL evaluation using model results in a 10-year (1991-2000) average hydrology period, in which the current climate condition was used. This study will analyze water quality of the estuary in a modified 1991-2000 hydrology due to sea level rise and warming. Three types of climate change scenarios will be conducted: 1) a 0.5-m Sea Level Rise (SLR) scenario, 2) a warming (GW, global warming) scenario (e.g., about 1.5-2^{o}C increase in monthly air temperature), and 3) a combined Sea Level Rise and Warming (SLR+GW) scenario. In these three scenarios, the watershed load will be the same as that in the 1991-2000 calibration of the WQSTM under the current climate condition. The differences in results are therefore related to altered estuarine hydrodynamics. Besides the impact on estuarine circulation and water quality due to changes in sea level and air temperature, the watershed nutrient loading would also be changed in the 2050 climate condition. Therefore, additional model scenarios will also be analyzed that include changes in watershed loads due to an altered climate in 2050 and use the estuarine hydrodynamics with or without sea level rise and warming.

2. Method

This work uses an estuarine model to estimate water quality responses to sea level rise and warming. A proper setting of the model is critical. The following describes the related methods.

2.1. The estuarine hydrodynamic and water quality model

The WQSTM, a coupled 3-dimensional CH3D hydrodynamic model and CE-QUAL-ICM water quality and sediment transport model [14] was used. The CH3D model simulates hydrodynamic circulation, which will be impacted by changes in either sea level or water temperature. The WQSTM model grid utilizes a z-type depth structure. The model grid has up to 19 layers depending upon the depth of water, and the thickness of each layer is fixed. The thickness of the surface layer is 2.13 meters (i.e., 7 feet), and the thickness of other layers is 1.53 meters (i.e., 5 feet). The model grid consists of 11,064 surface cells, and a total of 56,920 cells. The model boundary with the ocean is adjacent to the Bay mouth, and extends 10 km out to the ocean. The model calibration run is called the Base Scenario as a reference to analyze changes in estuarine conditions due to climate scenarios.

2.2. Model setting of water elevation at ocean boundary

The water elevation at the ocean boundary for model calibration in 1991-2000 was based on the observed hourly water level at the Chesapeake Bay Bridge Tunnel (CBBT) station (Fig. 1). For the sea level rise scenario, a necessary simplifying assumption presumed that tidally influenced fluctuations of hourly water level in the 10-year hydrology period would be approximated by the observed hourly water level fluctuations in 1991-2000. Under this assumption, the water level rise in the estimated 0.5-meter sea level rise condition can be accomplished in the simulation by increasing the vertical depth of the model grid by 0.5 meters, while still using observed hourly water elevations for the boundary.

There are three potential methods by which the model grid depth can be increased by 0.5 m. One method involves adding an additional layer of 0.5 m below the surface layer. The second method involves adding an additional layer of 0.5 m below a layer other than the surface layer, such as the bottom layer. The third method available would increase the surface layer by 0.5 m.

The second method involves significant modification of the algorithm for horizontal transport, because there would be different thicknesses of water in the same model layer throughout the model domain. The first method still involves a reconstruction of linkages among faces of the model grid, modification of source code, and an associated slowdown in computation, but is easier to implement than the second method. The difference in depth resolution in the first layer between the first and third methods is only a quarter of a cell thickness. The two methods of grid modification produced insignificant differences [9]. Because the third method is easy to implement and yields results comparable to the first method, the third method was adopted.

2.3. Salinity simulation and model settings of salinity boundary conditions

The model computes 3-D salinity fields in the following way [15]:

$$\frac{\partial(S)}{\partial t} = -R_O\left(\frac{\partial(uS)}{\partial x} + \frac{\partial(vS)}{\partial y} + \frac{\partial(wS)}{\partial z}\right) + \frac{Ek_H}{\mathrm{Pr}_H}\left(\frac{\partial(K_H \partial(S)/\partial x)}{\partial x} + \frac{\partial(K_H \partial(S)/\partial y)}{\partial y}\right) + \frac{Ek_V}{\mathrm{Pr}_V}\frac{\partial(K_V \partial S/\partial z)}{\partial z} \quad (1)$$

Where,
S = salinity;
z = thickness;
u, v, w = x, y, z component of velocity
Ro = Rossby number
K = turbulent eddy coefficients (horizontal or vertical: H, v)
Ek = Ekman number (horizontal or vertical: H, v)
Pr = Prandtl number (horizontal or vertical: H, v)

The salinity at the ocean boundary for model calibration in 1991-2000 was based on bi-weekly observations at three monitoring stations, CB7.4, CB7.4N, and CB8.1E, at the Bay mouth (Fig. 1). Due to the influence of freshwater, the salinity at the Bay mouth is lower than that in the pelagic ocean. Sea level rise increases salt intrusion to the Bay from the ocean, increasing the salinity at the Bay mouth [13]. An adjustment of salinity at the ocean boundary is needed in the simulation of sea level rise. The

model simulation of 0.5 meter sea level rise by Hong and Shen [13] used a model grid with a boundary in the pelagic ocean, 100 km away from the Bay mouth. The salinity changes in the Chesapeake estuary, including at the mouth, in the current condition and the 0.5 meter sea level rise condition were estimated for hydrology years 2001 and 2003 by Hong and Shen [13], as well as 2000 (Shen, personal communication). In courtesy of Shen's detailed information, we adjusted salinities at the WQSTM boundary near the Bay mouth for a 0.5 m sea level rise scenario [9]. The adjustment was conducted by trial testing the boundary salinity modifications for the sea level rise simulation using the WQSTM, and simulated salt intrusion results were obtained, similar to Hong and Shen [13] for hydrology years 2000, 2001, and 2003 with a 0.5 m increase in sea level rise. This work uses the same method employed by Wang et al. [9] to set salinity at the boundary for 1991-2000 hydrology in the Sea Level Rise Scenario. The modifications to the ocean boundary involved three steps: 1) projecting bi-weekly observed salinity values recorded in the centroid of cells in the normal Base Scenario grid to the new Sea Level Rise Scenario grid with increased total depth, 2) calculating salinity values at the centroid of cells of the new grid, and 3) increasing salinity by 0.4 ppt. The salinity adjustment is also consistent with the salinity increase at the Bay mouth in sea level rise scenarios completed by Hilton et al. [12].

2.4. Key parameters used in water temperature simulation

Circulation in the estuary also redistributes water temperature in model cells, which is simulated in a manner similar to the salinity computation (Equation 1). Other than advection in tidal waters, thermal diffusion and heat exchange between air and water is the main process used to increase water temperature in the WQSTM simulation under warmer conditions. Changes in temperature due to the air-water exchange is considered proportional to the temperature difference between the water surface and a theoretical equilibrium temperature [16]:

$$\partial Tw / \partial t = K (Te - T)/ (\rho Cp dZ) \quad (2).$$

Where:

Tw=water temperature;
Z= depth
Te: Equilibrium temperature
K: heat exchange coefficient (Watt m^{-2} $C^{o\,-1}$)
Cp: specific heat of water (4200 Watt sec kg^{-1} $C^{o\,-1}$)
ρ: water density (1000 kg m^{-3})

For a water temperature simulation in the 2050 Warming Scenario, it is essential to estimate air temperature, as well as the theoretical equilibrium temperature (Te) and heat exchange coefficient (K) in year 2050.

2.5. Estimate of 2050 air temperature

Air temperature will increase by 2050 due to global warming [7, 10]. The air temperature in 2050 was estimated based on averaged values from six global circulation model (GCM) scenarios from phase 3 of the Coupled Model Intercomparison Project (CMIP3). The six GCM scenarios were: 1) bccr_bcm2_0, i.e., BCM2.0 of BCCR (Bjerknes Centre for Climate Research, Norway), 2) csiro_mk3_0, i.e., Mk3.0 of CSIRO (Commonwealth Scientific and Industrial Research Organization, Australia), 3) csiro_mk_3_5, i.e., Mk3.5 of CSIRO, 4) inmcm3_0, i.e., CM3.0 of INM (Institute for Numerical Mathematics, Russia), 5) micro3_2 i.e., MIROC3.2 of NIES (National Institute for Environmental Studies, Japan), and 6) ncar_ccsm3_0, i.e., CCSM3 of NCAR (National Center for Atmospheric Research, USA). Monthly temperature changes between 1995 (the simulation midpoint year used to establish the Chesapeake TMDL) and 2050 conditions were estimated [17, 18]. After noting abrupt changes between December and January a running-three-month average method was used to smooth the data (blue diamonds in Figure 2b) and then adjust daily air temperatures for scenarios involving a warming climate. The increase of monthly air temperatures for 2050 in this work ranges from 1.6 to 1.9^{o} C as shown in Figure 2b (blue dots).

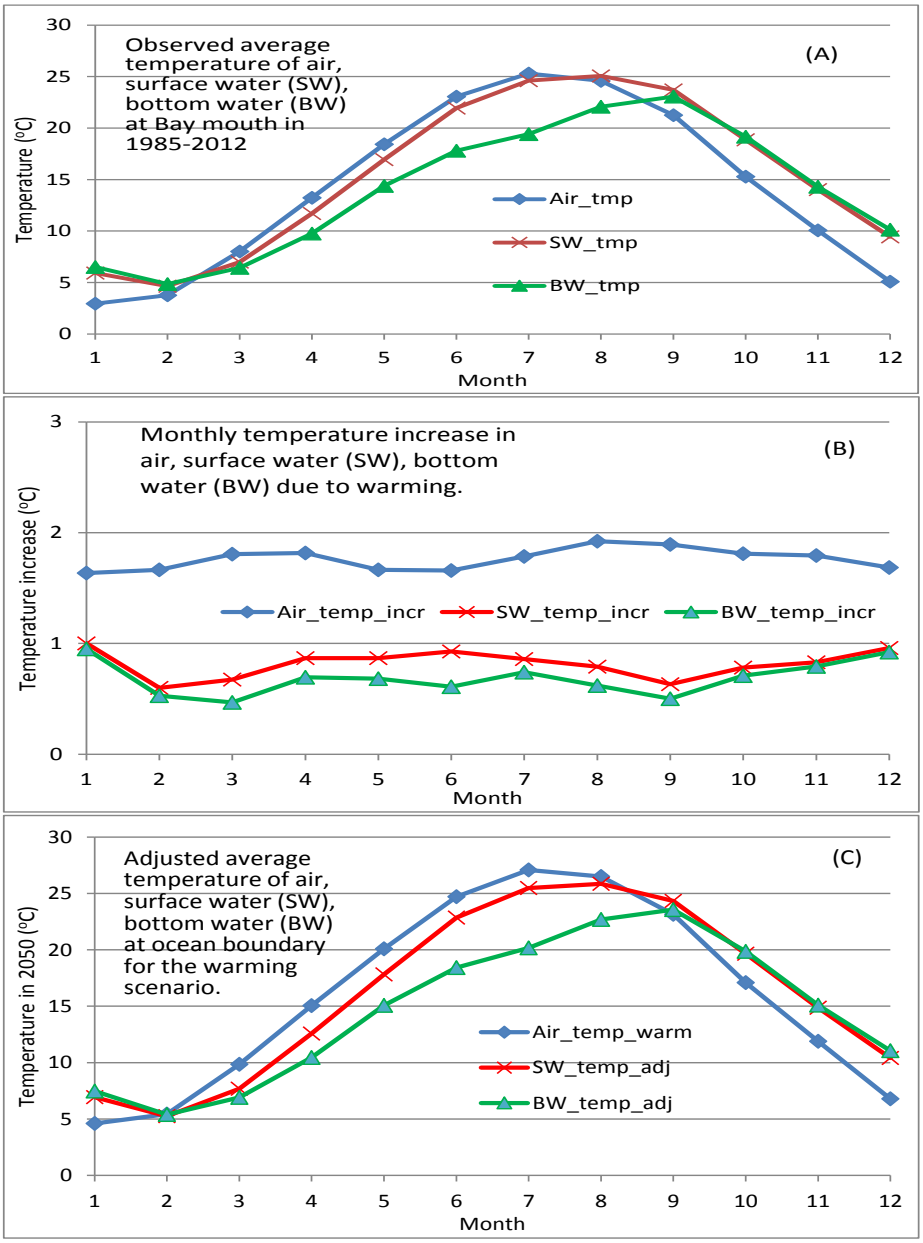

Figure 2. Illustration of adjustments of monthly water temperature at the boundary due to changes in air temperature in 2050. a) Observed average monthly temperatures of air, surface water, and bottom water at the Bay mouth from 1985-2012, b) increases of monthly temperature in the air, surface water, and bottom water due to warming in 2050, based on slopes of temperature changes in panel (a); c) averaged monthly temperatures in the air, surface water, and bottom water at the ocean boundary in the projected 2050 condition.

2.6. Simulation of water temperature in 2050

2.6.1. Te and K for simulation of water temperature in warming scenarios. The theoretical equilibrium temperature (Te) and heat exchange coefficient (K) are required to simulate water temperature (Equation 2). Te and K can be estimated from daily air temperature, dew-point temperature, or wet-bulb temperature, wind speed, and cloud cover or solar radiation [16, 19, 20]. By assuming no change in humidity for the same day in the Warming Scenario and the Base Scenario conditions and using the

estimated air temperature in the warming condition, a dew-point temperature for the Warming Scenario can be obtained. By further assuming no change in wind and cloud cover conditions in the warming and the base conditions, Te and K were calculated for the Warming Scenario. Using the estimated Te, K, and air temperature due to warming, water temperature in the Warming Scenario can be simulated.

The temperature of water changes more slowly than air temperature because water has a higher heat capacity. About one unit of heat energy is needed to warm the air one degree Celsius, while about four times more heat energy is needed to warm the water one degree Celsius. Morrill et al. [21] showed that water temperature in the upland streams of their study area increased by approximately 0.6° - 0.8° C for every 1° C increase in air temperature.

The Chesapeake estuary has a larger ratio of water volume to surface area than that of shallower rivers. For a 1° C increase in air temperature, there is expected to be a lesser temperature increase in the Bay's water than the stream estimates produced by Morrill et al. [21]. A simplified scoping warming scenario for the Chesapeake estuary was run with an increase in monthly air temperature of 1.6 - 1.9° C (Fig. 2b), which resulted in about 0.8- 1° C increase in the estuarine water, i.e., an approximate 0.5° C increase in water temperature for every 1° C increase in air temperature [9]. This result indicates that the CH3D simulation of water temperature and the estimated Te and K for the warming condition is acceptable. Note: in the simplified scoping warming scenario, the water temperature of the ocean boundary and freshwater inputs used the current climate condition. For more accurate calculations in warming scenarios, water temperature at the boundary and the input freshwater needed to be adjusted accordingly, and this point is addressed in the next two subsections.

2.6.2. Adjustment of water temperature at the ocean boundary. Figure 2a shows observed averaged monthly water temperatures at both the surface and the deepest bottom layer (about 18 meters deep) at the Bay mouth from 1985-2000, along with the observed averaged air temperatures from the Patuxent Naval Air Station. In high winter, the deep water had a higher temperature than the surface water, which in turn had a higher temperature than the air. In the summer, the air had a higher temperature than the surface water, which in turn had a higher temperature than the bottom water. The changes of air and water temperatures among months were nonlinear, showing hysteresis in the rising and falling limbs, consistent with observations made by Lee and Cho [22]. Based on the monthly change in air temperature (the blue diamonds in Fig. 2b) and considering slower changes in water temperature in comparison with changes in air temperature from the scoping warming scenario, relative changes in surface water and bottom water temperature in each month were calculated (Fig. 2b). These values were used to adjust the bi-weekly observed water temperature at the Bay mouth boundary for use in the warming scenarios (Fig. 2c).

2.6.3. Adjustment of water temperature in daily freshwater discharge. The model uses daily inputs of freshwater discharges. The increase of water temperature in rivers in the Warming Scenario can refer to the increases of temperature in the estuarine surface water (Fig. 2b, red crosses) with adjustment by a factor. Considering greater temperature changes in stream water compared to that in the estuary resultant from air temperature changes and referring to Morrill et al [21], a factor of 1.2 was applied to produce slightly greater increases of monthly temperature from stream water. These values were interpolated for daily temperature increments for freshwater discharged from the watershed in the warming scenarios.

2.7. Simulations of primary production, dissolve oxygen, and other water quality

The CE-QUAL-ICM water quality model simulates 36 state variables. They include various species of N-P nutrients and carbon as well as 3 grain sizes of fixed solids. Nutrient, light, and temperature dependent algal growth are simulated for three generalized groups, i.e., green algae, blue-green algae, and spring diatoms. A full carbon based simulation of DO that considers aeration, diffusion, mixing, temperature, algal activities, and processes involving materials of biological and chemical oxygen demand is also applied [14]. Transport forcing is provided by the CH3D hydrodynamic model. The daily constituent loads from the watershed are based on the simulation by the Chesapeake Bay Watershed

Model (CBWSM) Phase 6.0 [2] in the 1991-2000 calibration run that used actual climate conditions, land uses, and management practices in 1991-2000. Table 1 lists the estuarine model (WQSTM) scenarios applied in this study.

Table 1. List of scenarios and the modification of model settings.

Scenario name	**Depth of surface layer**	**Boundary salinity**	**T of ocean bound,**	**T of input freshwater**	**Heat exchange parameters**	**Watershed load**
Base Case Scenario	As initially designed	bi-weekly observations	bi-weekly observations	Daily, observations /calibration	Based on observed	Daily load from watershed model, calibrated for the years 1991-2000
Sea Level Rise Scenario (SLR)	Surface layer + 50 cm	readjust + increase	Same as the Base	Same as the Base	Same as the Base	
Warming Scenario (GW)	Same as the Base	Same as the Base	Increase, vary monthly	Increase, vary daily	Based on increased air T	
Sea Level Rise & Warming Scenario (SLR+GW)	Same as SLR	Same as SLR	Same as GW	Same as GW	Same as GW	
5% load increase (inf. 2050 load) Scenario	Same as the Base	Same as the Base	Same as the Base	Same as the Base	Same as the Base	5% increase in watershed loads compared to the Base, approximate the load in 2050.
5% load increase and SLR+GW Scenario	Same as SLR	Same as SLR	Same as GW	Same as GW	Same as GW	
10% load increase Scenario	Same as the Base	Same as the Base	Same as the Base	Same as the Base	Same as the Base	10% increase in watershed loads compared to the Base, resembling a worst possiblecondition in 2050.
10% load increase and SLR+GW Scenario	Same as SLR	Same as SLR	Same as GW	Same as GW	Same as GW	

A Base Scenario is based on the observed conditions in 1991-2000. It is the same as the calibration run and is used as a reference to analyze relative differences or changes in the estuarine water quality due to warming and/or sea level rise. The same watershed load used in the Base Scenario was also employed in three climate change scenarios: a Sea Level Rise Scenario (SLR), a Warming Scenario (GW, i.e., global warming), and a Sea Level Rise and Warming Scenario (SLR+GW).

Under the projected 2050 climate condition, due to global warming and modified precipitation and evapotranspiration, watershed loads would increase [17]. Compared to the Base Scenario, the loads of total nitrogen (TN), total phosphorus (TP) and total suspended sediment (TSS) from the watershed to the Bay were estimated to increase by 5 to 7 percent. Two additional scenarios for the estuary were run for 1991-2000, in which the watershed load was increased 5% to roughly represent estimates of 2050 watershed loads, but with different estuarine circulation patterns; one is identical to the Base scenario, and the other is the same as the SLR+GW scenario. Considering the potential influence of model errors motivated us to include two additional counterpart scenarios, in which the watershed loads were increased by 10%, in order to represent a dramatic change in conditions in 2050 for both aforementioned circulation scenarios.

3. Result and discussion

3.1. Response of circulation due to sea level rise and warming

This section uses the responses of salinity, temperature, and strength of stratification to analyse the influence on circulation by sea level rise or warming.

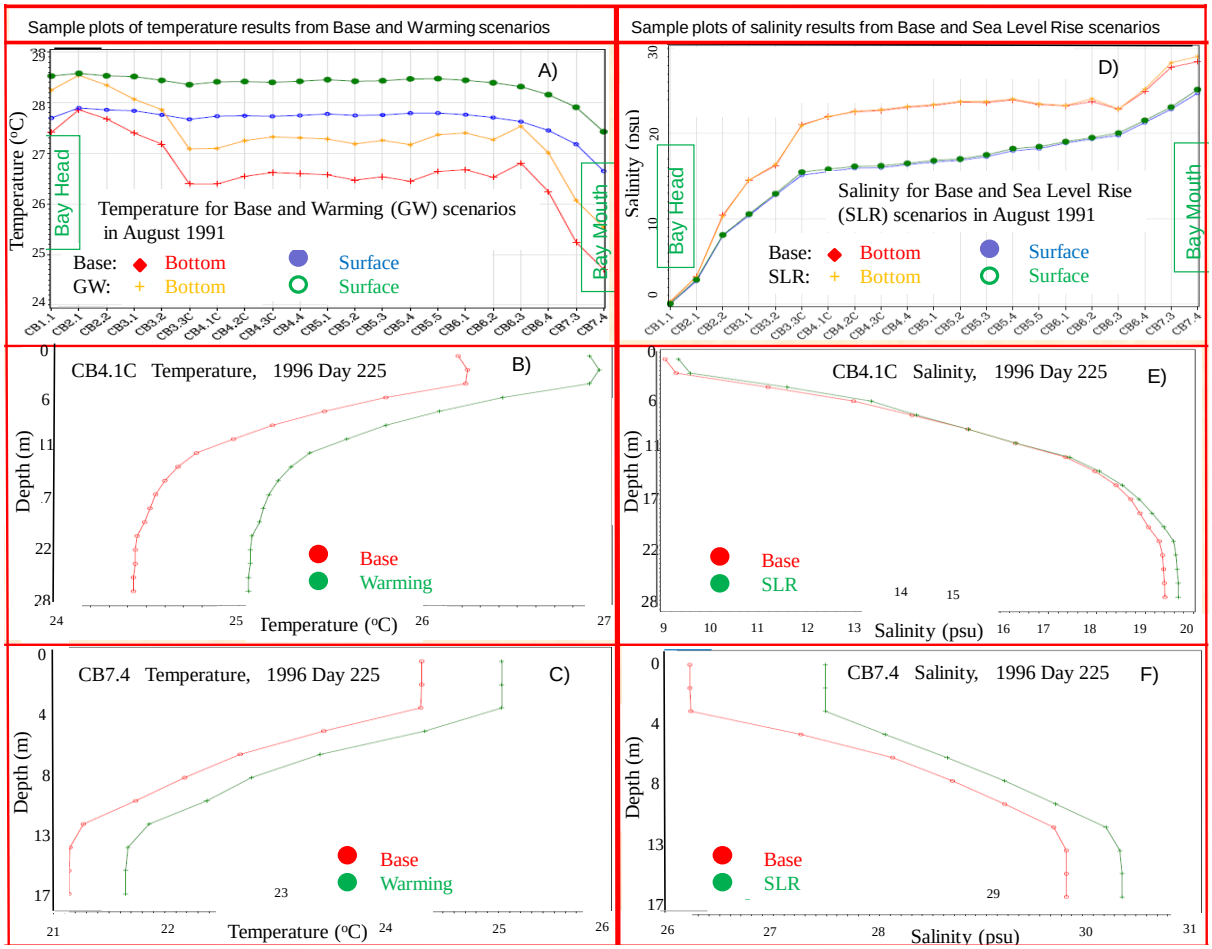

Figure 3. Sample results of temperature and salinity simulation in the Warming (GW) and Sea Level Rise (SLR) Scenarios. A) Temperatures of surface and bottom water in channel stations from the Bay head to mouth in Warming Scenario; B and C) Temperature profiles in stations CB4.1C and CB7.4; D). Salinity of surface and bottom water in channel stations from the Bay

head to mouth in Sea Level Rise Scenario; E and F) Salinity profiles in stations CB4.1C and CB7.4.

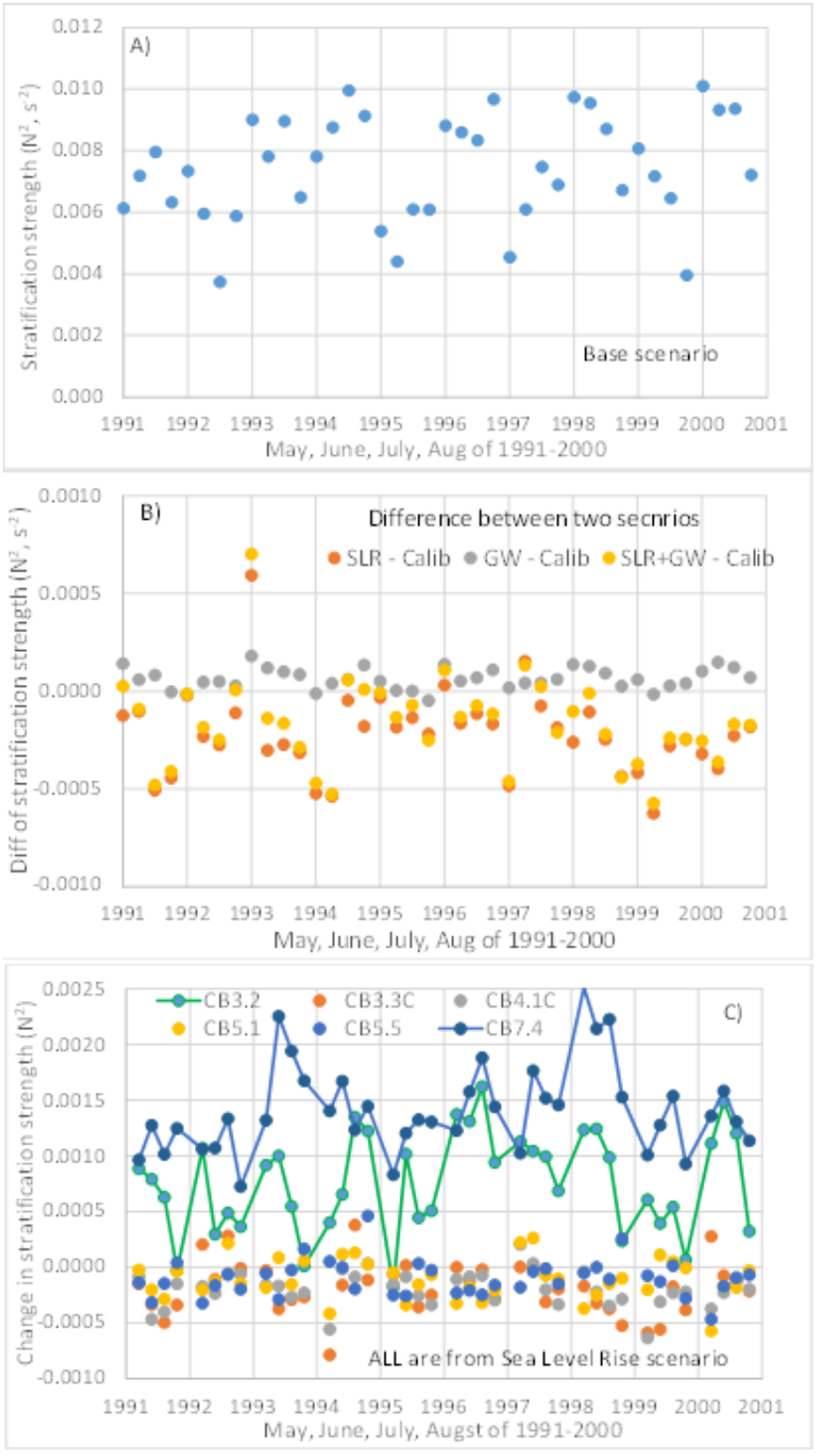

Figure 4. Stratification strengths in May, June, July and August of 1991-2000. A) stratification strength in CB4.1C in the Base Case Scenario; B) Difference of stratification strengths in CB4.1C between three climate scenarios and the Base Case Scenario; C) Difference of stratification

strengths in selected channel stations between the Sea Level Rise scenario and the Base Case Scenario.

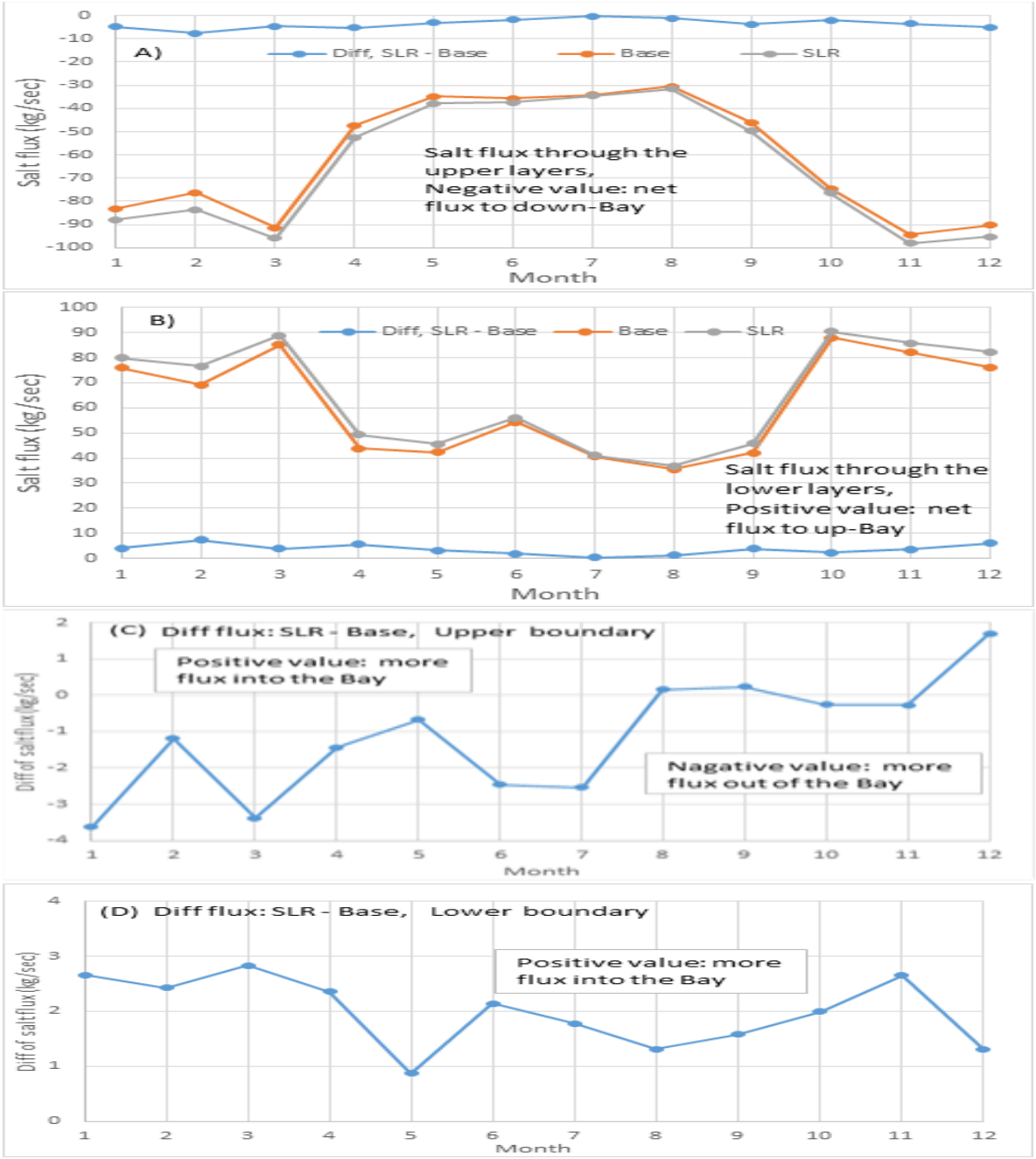

Figure 5. Monthly salt flux in the Base Case Scenario (orange) and the Sea Level Rise (grey) scenarios, and difference of salt flux between the two scenarios (blue). a) through the upper layer at a mid-Bay cross section near CB5.1 (Fig. 1); b) through the lower layer at the mid-Bay cross section; c) through the upper layer at the Bay mouth; d) through the lower layer at the Bay mouth. Note: a positive sign denotes net flux is up-bay-ward to the north or into the Bay, and negative sign denotes net flux is down-bay-ward to the south or out of the Bay.

3.1.1. Response of water temperature and stratification strength by warming. The most significant physical impact produced by warming acts upon water temperature and then, second, stratification. Without sea level change, the Warming Scenario does not cause significant changes in salt flux and salinity in the Bay. Compared to the Base Scenario, the Warming Scenario (GW) caused both the bottom and surface water temperatures to increase by about 0.6 ^{o} -1^{o} C in the summer in all stations along the channel, from the Bay head to the Bay mouth (Fig. 3a). The increase in temperature is further evident from Figures 3b and 3c, which display temperatures at vertical profiles in 2 channel stations on an arbitrarily chosen summer day (August 12, 1996).

The stratification strength was assessed based on the square of the Brunt-Vaisala frequency, i.e., the N^2 value [23], at a maximum density gradient of a depth profile: $N^2=-(g/\rho)(d\rho/dz)$, where ρ is density, g is the acceleration of gravity, and z is depth. Heat exchanges with the air is the primary method by which water temperatures are increased in the Warning Scenario, and results in greater increases in water temperature for shallower depths in summer months. The density of the surface water was reduced to a greater extent under higher temperatures. This led to a greater density gradient and a greater stratification strength in the Warming Scenario compared to the Base Scenario, as shown in Fig 4b (grey dots) at station CB4.1C. The increase of stratification strength was also detected at other stations, e.g. CB2.2, CB3.1, CB5.1, CB6.1, and CB7.1. Accompanied with the warming, the depth of the maximum density gradient moved upwards in the water column to a slightly shallower position.

3.1.2. Response in salt flux, salinity fields, and stratification by sea level rise. Among the most significant physical impacts on the estuary produced by sea level rise are changes in salinity and stratification. Sea level rise slightly increases salt flux into the Bay. The change in monthly salt flux ranges from -1 to +3 kg/s. The increase of flux into the Bay by sea level rise occurs mainly through the boundary at deeper levels, which has positive influxes in every month (Fig. 5d), with greater influxes from late fall to early spring and lesser influxes from late spring to early fall. This pattern is reversed for the net flux through the upper boundary layers (Fig. 5c). In the winter and spring months the salinity at the boundary responds more sensitively to salt intrusion by sea level rise than the comparatively dryer seasons of summer and fall. Although elevated sea level retards the outflow of freshwater, the increased salt intrusion from lower layers generates an upwelling at the head of the salt wedge, and prompts a returned down-bay-ward force along the surface. This force exerted along the surface generates more outflow through the upper boundary. Overall, sea level rise promoted the two-layer estuarine circulation, which can be seen more clearly from a cross section of the salt flux through the mid-Bay (Fig. 5a-b), near station CB5.1 (Fig. 1). In the Base Scenario both the influx in the lower layer and the outflux in the upper layer were greater in the wetter winter-spring months than in the dryer summer months. Under a regimen of sea level rise, the monthly influxes in the lower layer increased (i.e., more positive, Fig. 5b) and, concordantly, the monthly outflux in the upper layer also increased (i.e., more negative, Fig. 5a). The changes in salt influx or outflux were greater in the winter-spring months than in the summer months.

Along with elevated salt intrusion due to sea level rise, the average bottom and surface salinity increases, as shown in Fig. 3d at monitoring stations along the channel, from the Bay head to the Bay mouth in an arbitrarily chosen summer. The salinity has a greater increase at the Bay mouth, e.g., CB7.4, Fig. 3f, than at the inner Bay (e.g., CB4.1C, Fig. 3e). Generally, salinity increases throughout the entire depth profile, but in some upper Bay stations there are occasions wherein (e.g. CB2.2 on August 8, 1994) the surface salinity may show a decrement (figure not shown). These decrements can be attributed to conditions a few days prior to specific events. In this instance (August 8, 1994) dry conditions and a lack of freshwater discharge contributed to strong salt intrusion in the Base Scenario, but the Sea Level Rise Scenario did not generate enough salt intrusion on that day to greatly affect the surface water salinity near the Bay head.

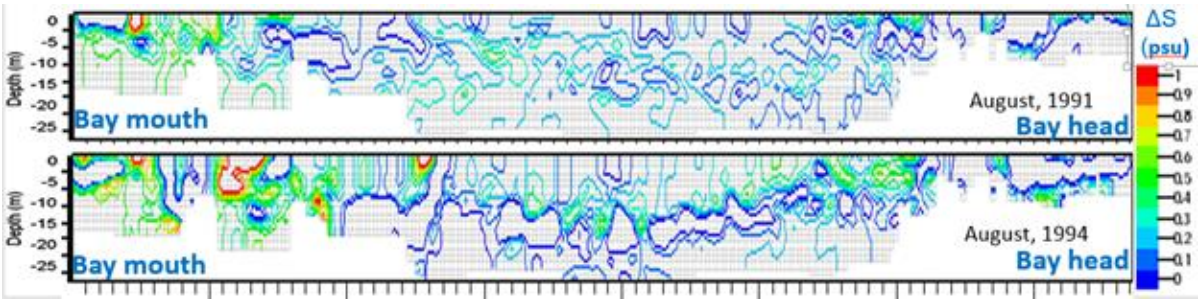

Figure 6. Change of salinity (ΔS, psu) along the channel of the mainstem Bay in August of 1991 and August of 1994 by 50-cm sea level rise versus the Base Case Scenario.

Figures 6a and 6b are contour maps of salinity difference between the sea level rise and the Base Scenario along the mid channel from Bay mouth to Bay head in August of 1991 and 1994, respectively. Under the same amount of salt intrusion with sea level rise, the relative increase, i.e. percent increase, compared to the Base Scenario, of salinity in a wet time period, e.g. August 1994, are greater than that in a normal or dryer time period, e.g. August 1991. Thus, the changes in salinity are greater in August 1994 (Fig. 6b) than those in August 1991 (Fig. 6a), which is in agreement with model experiments conducted by Hong and Shen [13]. In both cases, salinity increases more in the mid-depth (at about 10 m where pycnoclines usually occur) than in the surface or bottom layers. There, the maximum density gradient in the Base Scenario condition was mostly situated around the upper boundary of the pycnoclines, at somewhat less than 10 m. In the Sea Level Rise Scenario, the depth of greater salinity increases is below the maximum density gradient, thereby increasing stratification strength in most places.

However, in deep regions that have a deep channel designated-use such as CB4.1C, the maximum density gradients in the Base Scenario for such a location lies at approximately 12 m in depth at most times of the simulated summer periods, near the lower boundary of the pycnocline. The simulated increase of salinity at the aforementioned mid-depth (about 10 meters) above the usual location of the maximum density gradient reduces the overall density gradient, thus the stratification strength is reduced. Accordingly, in most of the simulated summer months in the Sea Level Rise Scenario, stratification strength in CB4.1 decreases (Fig. 4b), while in a few months, such as August 1994, the stratification increases. The response of stratification strength to sea level rise in the deep stations near CB4.1, like CB5.1, is similar (Fig. 4c). However, in most other channel stations (such as CB3.2 and its northern stations, CB7.4 and CB6.1 and its southern stations) the sea level rise caused stratification strengths in most months to increase (Fig. 4c). The aforementioned phenomena in these stations have the potential to change when freshwater discharge is significantly altered.

3.1.3. Response of stratification strength by combined sea level rise and warming. In comparison with the Base Scenario, stratification at station CB4.1 in the Sea Level Rise and Warming (SLR+GW) Scenario decreases in most cases, but is slightly greater than that in the Sea Level Rise Scenario (Fig. 4b). This indicates that the impact on stratification is mainly controlled by sea level rise, and less so by temperature change.

3.2. Impact on phytoplankton, dissolved oxygen and water clarity by sea level rise and warming

Chlorophyll-*a*, DO and water clarity are three key water quality components in the Chesapeake Bay TMDL (USEPA, 2010). This section analyzes their responses to warming and sea level rise.

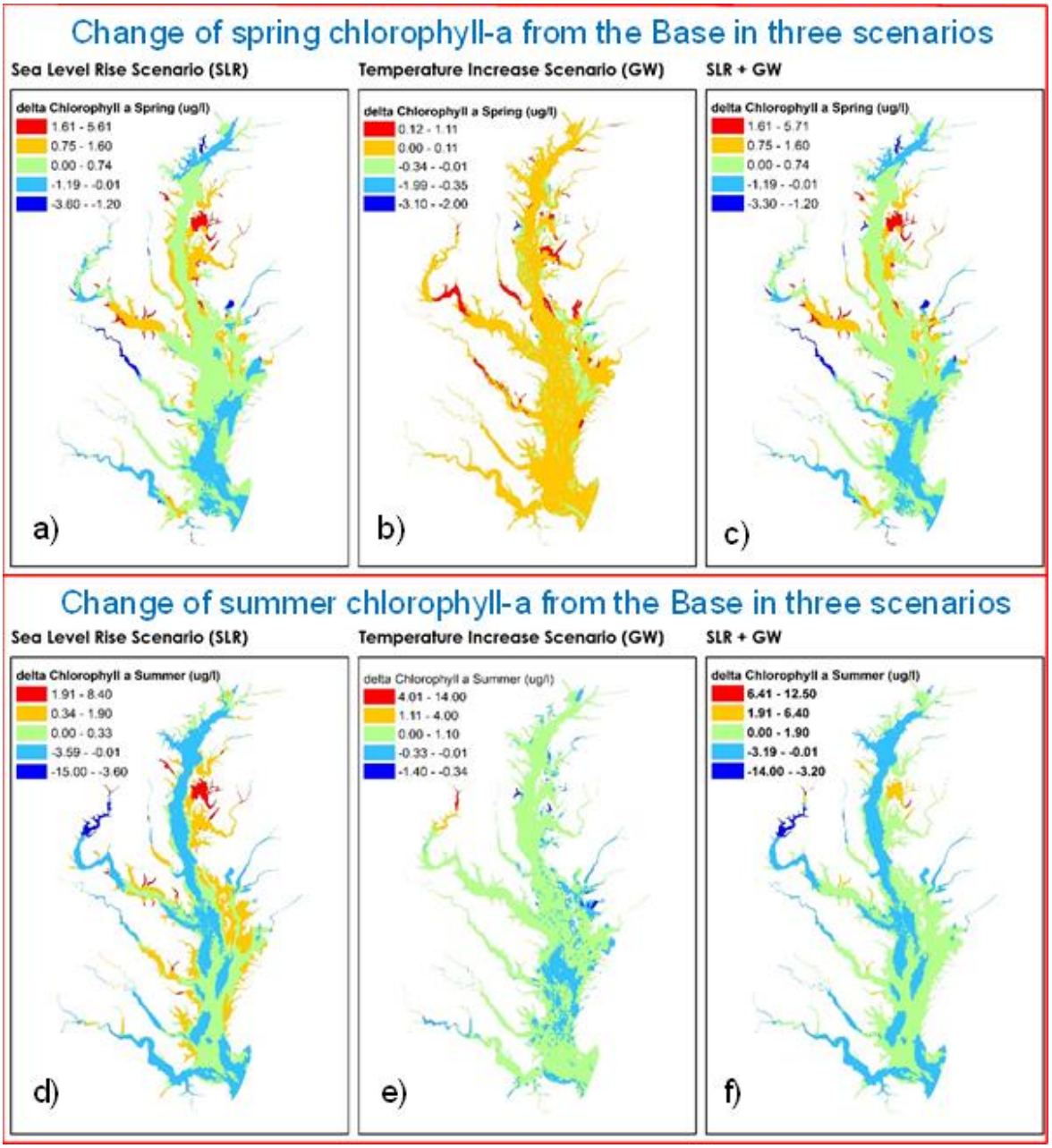

Figure 7. Change of spring and summer chlorophyll-*a* concentrations in three climate scenarios from the Base Scenario. A) spring ΔChl (SLR Scenario - Base Scenario); B) spring ΔChl (Warming Scenario - Base Scenario); C) spring ΔChl (Sea Level Rise and Warming Scenario - Base Case Scenario); D) summer ΔChl (Sea Level Rise Scenario - Base Case Scenario); E) summer ΔChl (Warming Scenario - Base Case Scenario); F) summer ΔChl (Sea Level Rise and Warming Scenario - Base Scenario).

Figure 8. Response of surface chlorophyll-*a* (a-c), inorganic suspended solids (ISS) (d-f), total suspended solids (TSS) (g-h) and diffused light attenuation coefficient (Kd) (i-j) in mainstem segments. a) Spring and summer chlorophyll-*a* in the Base Scenario, b) changes of spring chlorophyll-*a* by three climate scenarios compared to the Base Scenario, and c) changes of summer chlorophyll-*a* by climate scenarios compared to the Base Scenario; d) Spring and summer ISS in the Base Case Scenario, e) changes of spring ISS by climate change scenarios compared to the Base Scenario, f) changes of summer ISS by climate change scenarios compared to the Base Scenario. Surface water total suspended solids (TSS) concentration and diffused light attenuation coefficient (Kd) in mainstem segments. g) Spring and summer TSS in the Base Scenario, h) changes of TSS by sea level rise; i) spring and summer Kd in the Base Scenario, j) changes of Kd by sea level rise.

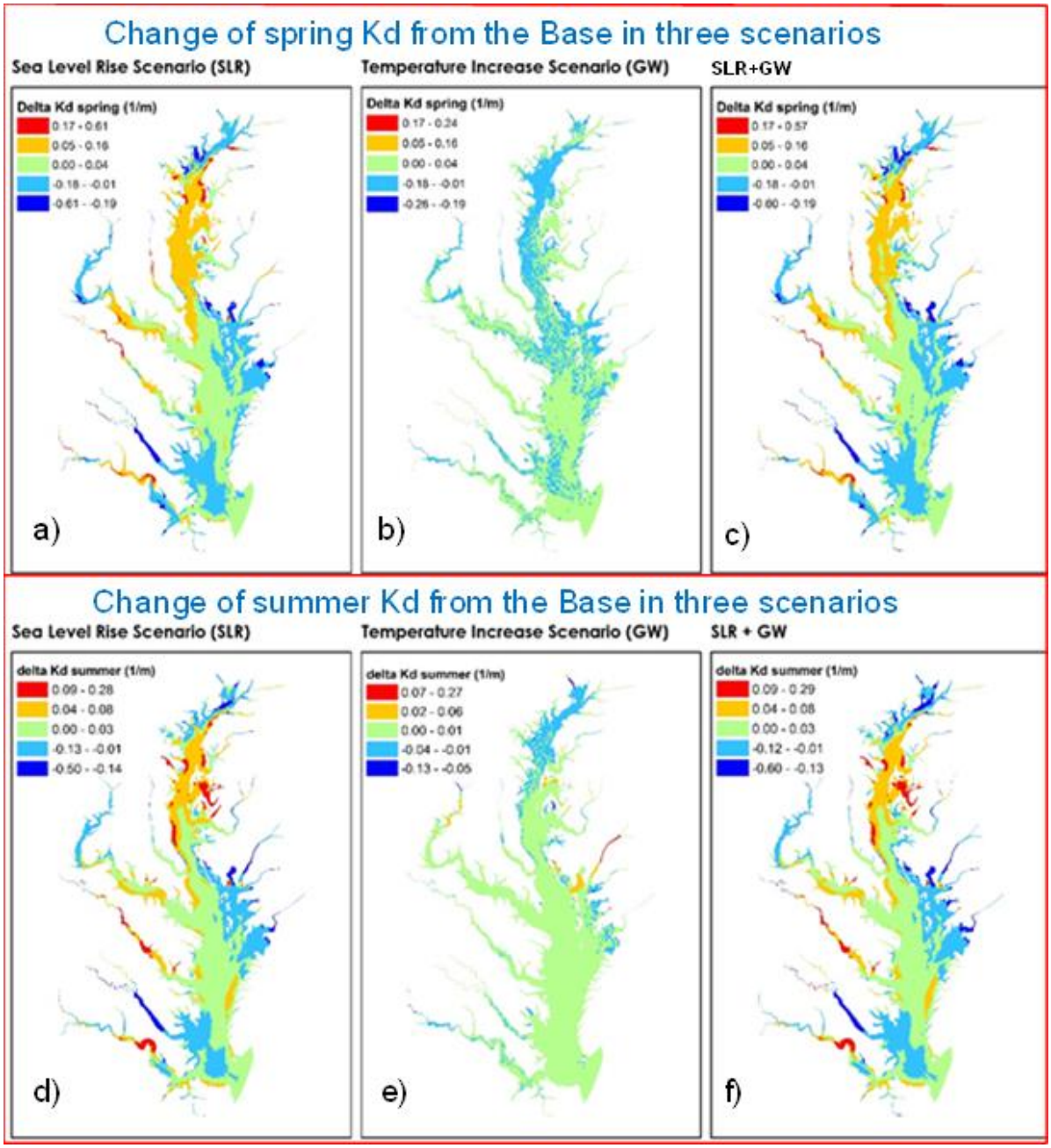

Figure 9. Change of spring and summer Kd in three climate scenarios compared to the Base Scenario. A) spring ΔKd (Sea Level Rise Scenario - Base Case Scenario); B) spring ΔKd (Warming Scenario - Base Case Scenario); C) spring ΔKd (Sea Level Rise and Warming Scenario - Base Scenario); D) summer ΔKd (Sea Level Rise Scenario - Base Scenario; E) summer ΔKd (Warming Scenario - Base Scenario); F) summer ΔKd (Sea Level Rise and Warming Scenario - Base Scenario).

3.2.1. Impact of water quality by warming. Increase of temperatures in the spring increases metabolism of algae. In the Warming Scenario spring chlorophyll-a concentration increases broadly in the estuary. However, the increase is only slight, ranging from 0 - 0.11 µg/L (Fig. 7b), and is approximately a 0.01 µg/L increase in most areas (note: not scaled in the map). Only in areas closest to freshwater inputs (which are more influenced by warmed terrestrial sources of water) is the increase of chlorophyll-a greater than 0.11 µg/L. The response of summer chlorophyll-a is similar to that in the spring, with

slightly greater increases in summer chlorophyll-a (Fig. 7e), around 0.02 μg/L increase in most areas. These can also be seen from Fig. 8 (b and c) (orange dots). The average chlorophyll-a concentration in the upper- and middle-Bay increases slightly, i.e., 0.03 percent and 0.12 percent in the spring and summer, respectively (Table 2).

Table 2. Summary of relative changes in anoxic volume, average surface chlorophyll, and Kd in the upper and middle Bay by climate change scenarios versus the Base Case Scenario.

Scenario name	Watershed load	Estuarine circulation	Summer anoxic volume (% change)	Spring surface chlorophyll (% change)	Summer surface chlorophyll (% change)	Spring surface Kd (% change)	Summer surface Kd (% change)
Base Case	Present	Present	---	---	---	---	---
SLR (Sea level rise)	Present	SLR	-14.4%	1.93%	-1.23%	1.23%	1.15%
GW (Global warming)	Present	GW	2.26%	0.03%	0.12%	-0.245%	-0.21%
SLR+GW	Present	SLR+GW	-11.6%	1.84%	-1.07%	0.85%	0.81%
5% increase of load	1.05 times the Base	Present	9.65%	2.51%	2.27%	0.72%	0.52%
5% increase of load, and SLR+GW	1.05 times the Base	SLR+GW	-2.12%	4.80%	1.34%	1.60%	1.38%
10% increase of load	1.1 times the Base	Present	18.7%	4.750%	4.26%	4.81%	3.35%
10% increase of load, and SLR+GW	1.1 times the Base	SLR+GW	6.35%	6.95%	3.21%	5.67%	4.14%

Light attenuation by water (denoted by Kd as the diffused light attenuation coefficient) is a function of concentrations of chlorophyll-*a* and other organic particulates, inorganic suspended solid (ISS) and color of dissolved organic matter [24]. The warming climate increased chlorophyll-*a*, leading to increased Kd. However, the increased temperature of surface water decreased its density and increased the settlement of fine ISS, e.g., clays and silts, thereby decreasing ISS concentration in the surface layer (Fig. 8, e and f, orange dots). Kd increased slightly in the spring and summer in mid and lower Bay in the Warming Scenario (Fig. 9, b and e), where the changes in chlorophyll-*a* were the main causes of changes in Kd. However, in the upper Bay closer to the mouth of the Susquehanna River, which was influenced significantly by terrestrial water inputs (segments CB1TF and CB2OH), the influences warming water had on increasing sinking rates of ISS became more important in controlling changes in Kd, and drove decreases of Kd. The average Kd in the mainstem Bay decreased by about 0.2 percent in the spring and summer in the Warming Scenario (Table 2).

There are three main physical and chemical processes related to warming that influence the Bay's anoxia: 1) the increased water temperature increases respiration and oxygen consumption, 2) the increased stratification (Fig. 4b, grey dots) helps to retain the anoxic condition, and 3) increased temperature reduces oxygen solubility and DO concentrations. Biologically, warming helps algal blooms in the spring and summer (Fig. 7, b and e), and results in higher biological oxygen demands. Compared to the anoxic volume in the Base Scenario, the influence on anoxia by the stated physiochemical and biological processes is small, thus there is only an increase in anoxic volume of

1.34% produced by the Warming Scenario (Table 2 and Fig. 10). Figure 11 is a GIS plot of difference in DO (ΔDO), between a climate change scenario and the Base Scenario in water greater than 12 meters in depth. In the Warming Scenario, ΔDO decreases in most areas (Fig. 11b), consistent with the increases of spring and summer chlorophyll-*a* (Figs. 7 (b & e) and 8 (b & c)). The algae produced in the surface water of a segment may drift to other segments before they settle and decay in bottom layers. Therefore, changes in bottom DO are not always consistent with changes in surface chlorophyll-*a* [25]. The ΔDO has certain degrees of variability over these areas. The factors driving an increase of DO in the area near the Bay mouth is unclear, but may be due to warmer sea water on the bottom that reduces stratification.

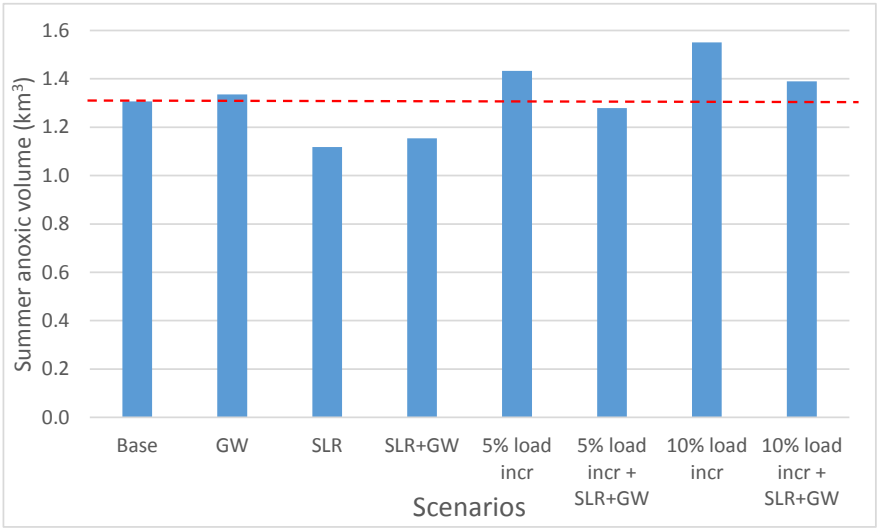

Figure 10. Summer average anoxic volume (km^3) from the Base Scenario and climate change scenarios.

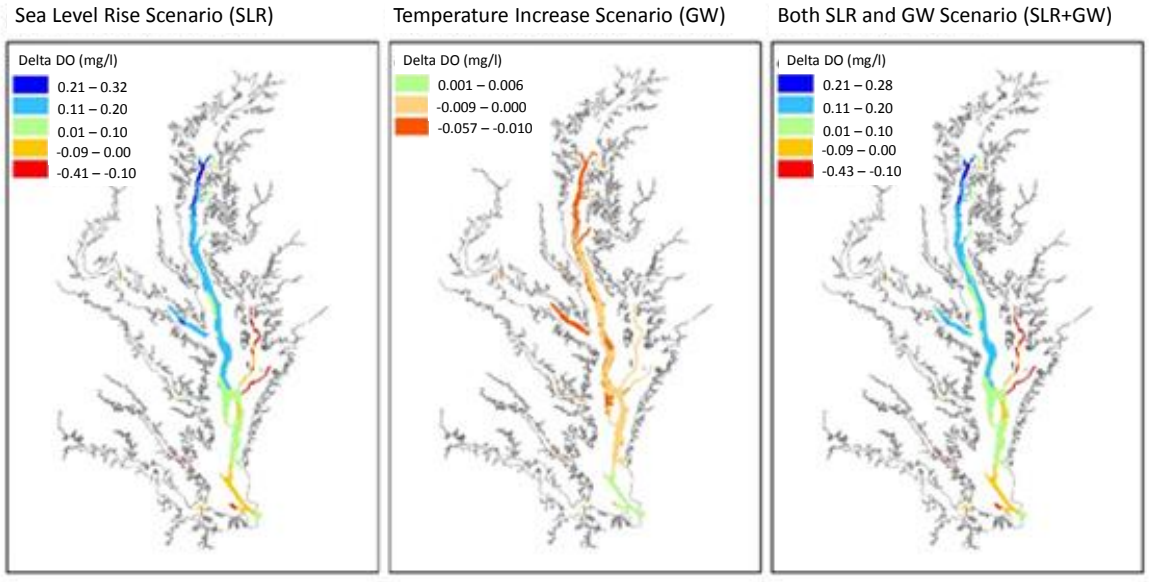

Figure 11. Change of summer DO concentration (ΔDO, mg/L) for water depth>=12 m in three climate scenarios from the Base Case Scenario. A) ΔDO (Sea Level Rise Scenario - Base Scenario); B) ΔDO (Warming Scenario - Base Scenario); C) ΔDO (Sea Level Rise and Warming Scenario - Base Scenario).

3.2.2. Impact on water quality by sea level rise. Nutrients and light are two main limiting factors of algal growth in the Chesapeake, while light attenuation is dependent upon concentrations of ISS, chlorophyll-a, and other matter that determine water clarity. Sea level rise influences transport and redistributes the concerned components among CB segments. Comparing these components together can help to better understand the influences of sea level rise on water quality.

(A) Response in transport of suspended solids and water clarity in sea level rise

The influence on circulation by sea level rise affects transport of inorganic suspended solids. In the Base Scenario, the surface ISS decreases rapidly from the Bay head to the Bay mouth (Fig. 8d) as settling continues during down-Bay ward transport. Concentrations of ISS at the Bay mouth (e.g., CB7.4) are slightly greater than those in inner stations, e.g., CB7.3, due to the oceanic source.

In the shallow fresher areas (i.e., the tidal fresh and oligohaline environments) of the upper Bay, the slower downstream transport of fresh water in the Sea Level Rise Scenario documented by Hong and Shen (2012) generates a greater volume of water than that observed in the Base Scenario and reduces ISS concentration in segments C12TF, C11TF, and CB2OH (Fig. 8e and 8f, blue dots). Similarly, in the lower Bay near the Bay mouth (e.g., segments CB6PH, CB7PH and CB8PH) the sea water intrusion also reduces ISS concentrations, though the influence is weak and the reduction of ISS concentrations is slight. However, in both the lower and upper Bay the increase in salinity from sea level rise may also benefit the suspension of fine ISS in surface waters and thereby increase ISS concentrations. Still, this may not be the key controlling factor in most of the lower and upper Bay areas; rather the increased surface water volume or changes in water movement may be more critical in determining ISS concentrations in the Sea Level Rise Scenario.

The situation is different in the deep water areas of the mid-Bay, such as that observed in segments CB3MH and CB4MH. There the increase in surface water volume becomes a less important factor, while the retention of materials in the Bay influenced by sea level rise becomes more important in governing ISS levels in surface water. Overall, surface ISS concentrations increase in the Sea Level Rise Scenario. In addition to a greater amount of material remaining within the Bay, the increased salinity increases water density and retards sinking of ISS from the surface.

TSS consists of ISS and particulate organic matter. The distribution and patterns in changes of TSS among the CB segments in the Sea Level Rise Scenario (Fig. 8h, blue and orange dots) are similar to changes in ISS (Fig. 8, e-f, blue dots). This suggests that ISS is the main component of TSS, while the contributions made by changes in algae due to sea level rise are relatively small compared to the changes in ISS concentrations. The changes in Kd among the CB segments due to sea level rise (Fig. 8, j, blue and orange dots) have similar patterns as those found for TSS (Fig. 8h). The average spring and summer Kd in the upper- and middle-Bay increases by about 1.2 percent (Table 2).

(B) The response of chlorophyll-*a* to sea level rise

Changes in spring chlorophyll-*a* in the Sea Level Rise Scenario have greater ranges than those produced in the Warming Scenario (Fig.7a vs. 7b, or 8b blue vs. orange dots). In the mid-Bay area (segments CB3-CB5), the range of increases in the Sea Level Rise Scenario vary between 0.2-0.6 μg/L (Fig. 8b, blue dots). Spring chlorophyll-*a* decreases 0.1-0.3 μg/L in the upper and lower Bay, seen in segments C12TF, C11TF, CB2OH, CB6PH and CB7PH. Accompanied with the increased salt flux into the Bay, sea level rise facilitated the retention of nutrients in the estuary for a longer period of time, causing larger areas in the Bay, especially the mid-Bay, to grow more algae in the spring. Simultaneously, the increased influx from the ocean may dilute nutrient concentrations. This action is more prominent in areas nearer to the Bay mouth, where nutrient concentrations are relatively low and are more affected by ocean water dilution. Thus, spring chlorophyll concentrations in the lower Bay are decreased. The cause of decrease in chlorophyll concentration in the upper Bay is similar to the cause of decreased ISS concentrations, namely dilution produced by increased water volume in the upper Bay as a result of sea level rise [13].

In the summer, the response of chlorophyll-*a* to sea level rise in the CB segments (Fig. 8c, blue dots) is the reverse of that observed in the spring (Fig. 8b, blue dots), apparently to compensate for the nutrient

uptake occurring in the spring. The average chlorophyll-*a* concentration in the upper- and middle-Bay increases by about 2 percent in the spring, while decreases of 1.2 percent occur in the summer (Table 2). In the mid Bay (segments CB3MH and CB4MH) the excessive algal growth in the spring in the Sea Level Rise Scenario lessened the amount of nutrients remaining in the summer and reduced summer chlorophyll. In the upper Bay (segments C11TF and C12TF) and lower Bay (segments CB6PH and CB7PH), the weaker algal growth in the spring in the Sea Level Rise Scenario left more nutrients available in the summer, increasing summer chlorophyll. The segments between the two areas of increasing and decreasing chlorophyll-*a*, (e.g. CB2OH, VA5MH, and MD5M) do not show a reversed direction of change for chlorophyll-*a* between spring and summer. Because they are in transition between the areas of different trends in chlorophyll-*a* changes, their nutrient and chlorophyll-*a* concentrations are influenced by adjacent segments.

(C) Response of anoxic volume to sea level rise

Sea level rise increases residence times of nutrients and organic carbon in the estuary. This can promote algal blooms, increase oxygen demand, and increase anoxic volume. However, the anoxic volume in the simulated 10 summers of the Sea Level Rise Scenario were about 0.2-0.4 km^3 less (14.5 percent, Table 2) than those in the Base Scenario (Fig. 10). This suggests that the change in summer hypoxic conditions in the Sea Level Rise Scenario may be more closely related to alterations of physical processes rather than algal processes.

There are two physical processes in sea level rise that may reduce anoxic volume: A) The promoted salt intrusion in the lower layer (Fig. 5b) brings oxygen-rich sea water into the Bay's anoxic area, as is represented by the cross section near station CB5.1 at the mid-Bay. At this cross section, the variation of monthly oxygen influxes through the lower layer or the outward fluxes through the upper layer (Fig. 12, b and a) are consistent with the variation of salt fluxes (Fig. 5, b and a). Despite the increase of oxygen influx through the lower layer in the summer being less than that in the winter, such an increase can significantly reduce the Bay's anoxic condition. B) The reduced stratification in the anoxic center promotes mixing and increases bottom DO. It should be noted, as presented in Section 3.1, that sea level rise promotes estuarine circulation and increases the overall stratification in the Bay. However, in the Bay's anoxic center, i.e., the deep water region of segments CB3MH, CB4MH, and CB5MH, the increase in salinity at its maximum density gradients in most summer months was less than that produced at shallower depths, causing a reduction of stratification strength (Fig. 4c) and reducing anoxic conditions.

There are cases showing that the reduction of stratification in the anoxic center by sea level rise may not be the main driver in the reduction of summer anoxia. For example, 1996 had a relatively wet summer in the time period 1991-2000. The decrease of stratification in the anoxic center by sea level rise in 1996 was weaker than that in other years (Fig. 4). However, the reduction of anoxic volume in 1996 was not the lowest among the simulated 10 years (Fig. 13). In another instance, the reduction of anoxia by sea level rise is greatest in 1993 (Fig. 13), yet the decrease of stratification in the anoxic center was also not the greatest (Fig. 4). The years 1991, 1992, and 1997 all had relatively dry summers, and the Bay was relatively saltier. In these years, the salt influx in the Sea Level Rise Scenario was less than that seen in comparatively wetter years. The associated intrusion of oxygen-rich sea water to the Bay's anoxic center was relatively weaker, thus the anoxia reduction was less in these years than in other years (Fig. 13). In this case, salt water intrusion with relatively higher DO may have played an important role in reducing anoxia.

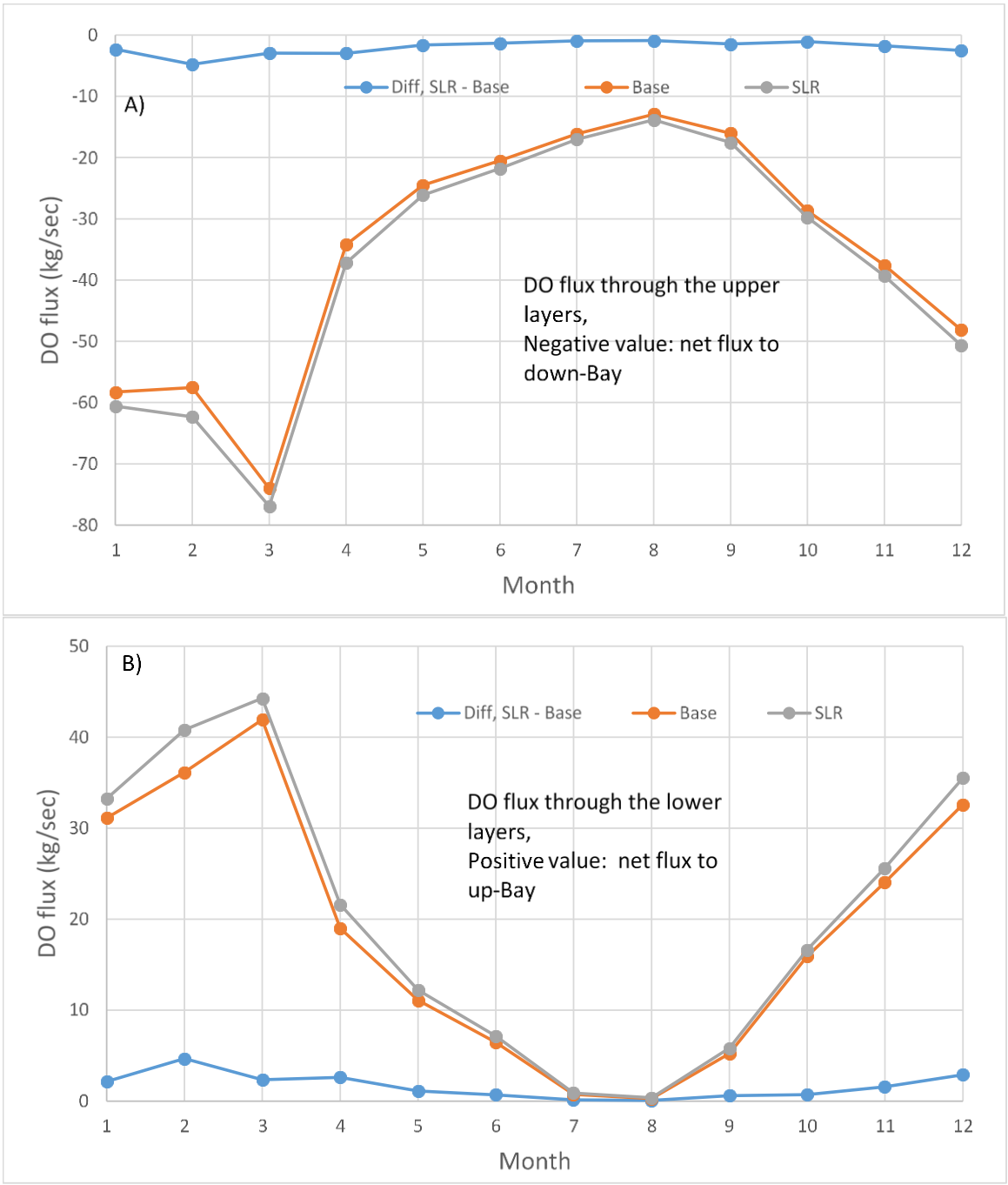

Figure 12. DO flux (kg/s) through the mid-Bay cross-section in the Base Case Scenario and Sea Level Rise Scenario. A) through the upper layers, B) through the lower layers.

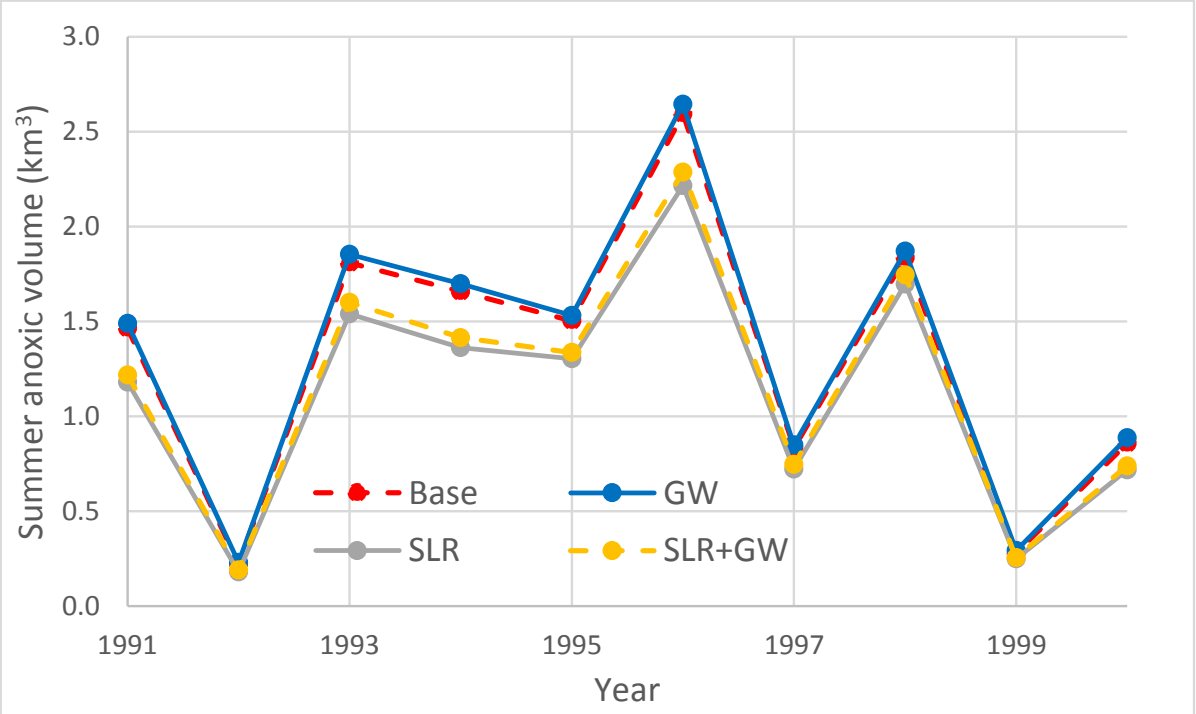

Figure 13. Summer anoxic volume of the mainstem Bay in the Base Case Scenario and three climate scenarios.

Summer hypoxic/anoxic volume reflects DO conditions in the bulk Bay. Still, changes in average DO concentrations in individual model cells can provide information on its spatial variation and provide some clues to analyze the related mechanisms. Figure 10a shows changes of average DO concentrations in water deeper than 12 m in the Sea Level Rise Scenario. Segments CB4MH, CB5MH, and CB3MH cover the Bay's anoxic center. There, DO is greater in the Sea Level Rise Scenario than in the Base Scenario. However, in segment CB7PH near the ocean boundary, DO is lower in the Sea Level Rise Scenario. Under the promoted bottom salt intrusion during the up-Bay-ward movement the particulate organic matter moved more slowly than the dissolved oxygen. Much of the particulates may remain in the lower Bay and continue to consume oxygen. Segment CB7PH is closer to the Bay mouth and has much greater DO than the anoxic zone. The relative change in DO by salt intrusion is not as large as that in the Bay's anoxic center. The oxygen consumption of the retained particulate organic matters plays a more important role in regulating DO in segment CB7PH, producing lower DO concentrations in the Sea Level Rise Scenario than the Base Scenario. The changes in DO concentrations during sea level rise are controlled by multiple factors, detailed analyses of which are beyond the scope of this paper.

(D) Influence on water quality by combined sea level rise and warming

The summer anoxic volume in the combined Sea Level Rise and Warming (SLR+GW) Scenario is 11.7 percent less than the Base Scenario (Table 2), but is slightly greater than the Sea Level Rise Scenario (Fig. 10). These findings suggest that the DO change in the Sea Level Rise and Warming Scenario compared to the Base Scenario is mainly influenced by sea level rise, while the influence of warming is small. The influence on chlorophyll-*a* (Fig. 8, b-c) and water clarity (referring to ISS, Fig. 8, e-f) of combined sea level rise and warming is also closer to that produced by sea level than that produced by warming.

3.3. Response of water quality due to increased watershed loads in a projected 2050 climate condition

Scenarios of a 5% increase in watershed loads (compared to the Base scenario) approximate the loading condition in 2050. The increase of nutrient loads causes an increase of spring and summer chlorophyll-a concentrations (about 2.4%) and light attenuation (about 0.6%) (Table 2). The increase in summer anoxia is mainly due to increased spring (January – May) nutrient loads, which has a high correlation with summer hypoxia and anoxia [25,26]. Under the same estuarine circulation as the Base Scenario, summer anoxic volume will increase by 9.65%, but is reduced slightly (-2.12%) when the estuarine circulation considers sea level rise (Fig. 10). The promoted oxygen-rich sea water intrusion by sea level rise has a greater influence on summer bottom DO than increasing phytoplankton concentrations in 2050 due to higher watershed loads or increasing temperatures.

Scenarios of a 10% increase in watershed loads are used to assess potential worst conditions in 2050. This scenario yielded about 4.5% increase of spring and summer chlorophyll concentrations and light attenuation (Table 2). Consistent with the scenarios using watershed loads of the Base condition, sea level rise and warming increases chlorophyll-a concentrations in spring and promotes greater light attenuation in the spring and summer and the retaining of suspended sediment in the Bay due to sea level rise, while less summer chlorophyll-a is produced due to the consumption of nutrients by algae in the spring. In scenarios of a 10% increase in watershed loads, summer anoxic volume increases by 18.7% when the estuarine circulation uses the Base condition, but only increases by 6.35% when sea level rise is considered for estuarine circulation. Thus, for management preparation in 2050, more nutrient controls than the current effort would be needed to reach water quality attainment goals.

4. Conclusions

In a projected warming condition of 2050 which employs an ensemble of GCMs estimating a 1.5-1.9^{o}C increase in monthly air temperatures, the water temperature in the Chesapeake Bay is estimated to increase by about 0.8-1^{o}C. The increased temperature promotes the metabolism of phytoplankton, leading to increases in spring and summer chlorophyll-*a* concentrations as well as increased oxidation rates, causing increased summer oxygen consumption and hypoxia. Our model experiment of a Warming Scenario results in lower summer DO in deep waters and greater anoxic volume. Besides the influence of algal growth in the warming condition, the increase of anoxia is also related to increases in stratification. The temperature of surface water increases more than temperatures at greater depths, resulting in lighter density in the surface layers which slightly increases stratification strengths.

In the 0.5 meter Sea Level Rise Scenario, due to the interactions of the increased sea water intrusion and fresh water outflow, the changes in nutrient retention varied among different Bay areas and CB segments. In some areas, spring or summer chlorophyll-*a* increases, while it simultaneously decreases in others. The changes in summer chlorophyll-*a* concentrations among the CB segments are reversed compared to the pattern of changes in spring chlorophyll, suggesting nutrient availability in the summer is related to algal consumption in the spring. In the Sea Level Rise Scenario, summer dissolved oxygen in deep water increases and anoxic volume is reduced. Sea level rise promotes estuarine circulation and increases oxygen-rich seawater intrusion, mainly through the lower layers, increasing bottom DO concentrations and reducing hypoxia. The stratification strengths in the majority of the Bay are increased under a scenario of sea level rise. However, in the Bay's anoxic center which has a Deep Channel designated-use, the maximum density gradient is primarily located near the lower boundary of the pycnocline. The larger increase of salinity in the pycnocline reduces the salinity gradient and weakens stratification. This promotes mixing of deep water and surface water, thereby reducing hypoxia. Combined with promoted oxygen-rich sea water intrusion in the Bay's anoxic area, sea level rise has an overall effect of reducing anoxia.

The combined Sea Level Rise and Warming Scenario also results in reduced anoxia, because the reduction of anoxia by sea level rise is much more significant than the increase of anoxia by warming in this model scenario.

A warming climate promotes algal metabolism and increases chlorophyll-*a*, leading to increased Kd. However, in the upper Bay closer to the mouth of the Susquehanna River, which is influenced

significantly by water inputs from terrestrial sources, the influences of warming water on sinking rates of ISS may be more important than the increase of chlorophyll-*a* to control changes in decreasing Kd.

Sea level rise's influence on circulation also affects the transport of inorganic suspended solids. In the simulated conditions, ISS is the main component of TSS and affects Kd, while the contributions by the changes in algal production are relatively small compared to the changes in ISS concentrations. In the upper Bay, accompanied with a slower downstream transport of fresh water in the Sea Level Rise Scenario, a greater volume of water than that observed in the Base Case Scenario reduces ISS concentrations in segments C12TF, C11TF and CB2OH, reducing Kd. In the deep water areas in the mid-Bay, the importance of increasing surface water volume becomes less important, while the retention of materials in the Bay due to sea level rise becomes more critical in governing ISS in surface waters. Therefore, we see ISS and Kd increases in the Sea Level Rise Scenario.

Overall, the estimated impact on the Bay's water quality is slight in the simulated warming condition if there is no nutrient load change; the impact on water quality is greater in our simulated 0.5 meter sea level rise. Under the condition of both sea level rise and warming, the water quality response to their combined effects and the changes in chlorophyll-*a* result in Kd and summer anoxia values that are closer to those produced by a condition of sea level rise. This indicates that in our simulated climate change condition, the influence on water quality is controlled to a greater extent by sea level rise than by warming.

The above impacts on water quality by the three climate scenarios were compared with the Base Scenario, and all scenarios used the same watershed loads as those in the current condition but utilized different estuarine hydrodynamics. The scenario of a 5% increase in nutrient loads due to climate change with no change in estuarine circulation (the Base Scenario condition) yielded a summer anoxic volume that was 10% higher than the Base Scenario condition. The scenario of a 5% increase in nutrient loads that also used a modified estuarine circulation due to sea level rise and warming yielded an extent of summer anoxic volume that was 2 percent less than the Base Scenario condition. This indicates that sea level rise can potentially benefit the reduction of summer anoxia and hypoxia. However, water quality relating to chlorophyll-*a* and water clarity will still be degraded. If watershed loads increase by 10% from their current condition, (a potential worst case for 2050) summer anoxic volumes would increase, from 6 to 19 percent, when using estuarine circulation in a sea level rise or current condition, respectively. Greater efforts are needed in controlling nutrient loads to prepare for the challenges of an altered climate in 2050. The estuarine water quality model used in this work does not simulate the function of wetlands in nutrient retention. Sea level rise may also contribute to an increased loss of wetlands that may negatively impact levels of DO, an important issue for management consideration that is not simulated in this work.

References

[1] USEPA (U.S. Environmental Protection Agency). 2010. *Chesapeake Bay Total Maximum Daily Load for Nitrogen, Phosphorus and Sediment*. U.S. Environmental Protection Agency Chesapeake Bay Program Office.

[2] Linker, C.L., R.A. Batiuk, G.W. Shenk, and C.F. Cerco. 2013. Development of the Chesapeake Bay Watershed Total Maximum Daily load allocation. JAWRA, 49: 986-1006More references

[3] CEC (Chesapeake Executive Council). 2009. C*hesapeake Bay Executive Order, 2009*, Annapolis, MD, USA.

[4] USACOE (U.S. Army Corps of Engineers). 2011. *Sea-level Change Considerations for Civil Works Programs.* Circular 1165-2-212. U.S. Army Corps of Engineers, Washington, DC

[5] Parris A., P. Bromirski, V. Burkett, D. Cayan, M. Culver, J. Hall, R. Horton, K. Knuuti, R. Moss, J. Obeysekera, A. Sallenger and J. Weiss. 2012. *Global Sea Level Rise Scenarios for the United States National Climate Assessment.* NOAA Technical Report OAR CPO-1. National Oceanic and Atmospheric Administration, Silver Spring, Maryland

[6] Sallenger, A.H., Doran, K.S., Howd, P.A., 2012. Hotspot of accelerated sea-level rise on the Atlantic coast of North America. Nature Climate Change 2, 884-888.

[7] Najjar, R.G., Pyke, C.R., Adams, M.B., Breitburg, D., Hershner, C., Kemp, M., Howarth, R., Mulholland, M., Paolisso, M., Secor, D., Sellner, K., Wardrop, D., Wood, R., 2010. Potential climate-change impacts on the Chesapeake Bay. Estuarine, Coastal and Shelf Science 86, 1-20.

[8] Walsh, J., Wuebbles, D., Hayhoe, K., Kossin, J., Kunkel, K., Stephens, G., Thorne, P., Vose, R., Wehner, M., Willis, J., Anderson, D., Doney, S., Feely, R., Hennon, P., Kharin, V., Knutson, T., Landerer, F., Lenton, T., Kennedy, J., Somerville, R., 2014. Chapter 2: Our Changing Climate. In: J.M. Melillo, T.C. Richmond, G.W. Yohe (Editors), Climate Change Impacts in the United States: The Third National Climate Assessment. U.S. Global Change Research Program, p. 19-67.

[9] Wang, P., L. Linker, H. Wang, C. Cerco, G. Bhatt and R. Tian (2014) Simulation of Chesapeake Bay Hydrodynamics for 2050 Climate Condition, Chesapeake Community Model Program Symposium, May 28-29, 2014, Annapolis, MD.

[10] Boesch, D.F., L.P. Atkinson, W.C. Boicourt, J.D. Boon, D.R. Cahoon, R.A. Dalrymple, T. Ezer, B.P. Horton, Z.P. Johnson, R.E. Kopp, M. Li, R.H. Moss, A. Parris, and C.K. Sommerfield. 2013. Updating Maryland's Sea-level Rise Projections. Special Report of the Scientific and Technical Working Group to the Maryland Climate Change Commission, University of Maryland Center for Environmental Science, Cambridge, MD. 22 pp.

[11] Johnson, Z., M. Bennett, L. Linker, S. Julius, R. Najjar, M. Mitchell, D. Montali, and R. Dixon. 2016. *The development of climate projections for use in Chesapeake Bay Program assessments.* STAC Publication Number16-006, Edgewater, MD. 52pp.

[12] Hilton, T. W., R. G. Najjar, L. Zhong, and M. Li. 2008. Is there a signal of sea-level rise in Chesapeake Bay salinity? J. Geophys. Res., 113, C09002, doi:10.1029/2007JC004247

[13] Hong, B. and J. Shen. 2012. Response of estuarine salinity and transport processes to potential future sea-level rise in the Chesapeake Bay. Estuarine, Coastal and Shelf Science, 104-105: 33-45

[14] More references Cerco, C.F., S.C. Kim, and M. Noel. 2010. The 2010 *Chesapeake Bay Eutrophication Model,* A report to USEPA Chesapeake Bay Program. US Army ERDC, Vicksburg, MS

[15] Johnson, B., R. Heath, B. Hsieh, K. Kim, and L. Butler. 1991. *User's guide for a three-dimensional numerical hydrodynamic, salinity, and temperature model of Chesapeake Bay*, Technical Report HL-91-20, Department of the Army Waterways Experiment Station, Vicksburg, MS

[16] Edinger, J. and J. Geyer. 1965. Heat exchange in the environment, Dept of Sanitary Engr and water resources, Research Project No. 49, The Johns Hopkins University, Baltimore, MD

[17] Bahatt G., Yactayo, G., Hinson, K., Claggett, P., Shenk, G., Linker, L., 2015. Towards an integrated climate change analysis of the Chesapeake Bay watershed. Abstract, Proc. Coastal and Estuarine Research Federation Biannual Conference, Seatle, WA.

[18] Wang, P., L. Linker, G. Bhatt, G. Yachato, and R. Tian. 2015. Accessing Impacts of 2050 Sea Level Rise and Temperature Increases on Chesapeake Water Quality. Abstract, Proc. Coastal and Estuarine Research Federation Biannual Conference, Seatle, WA.

[19] Edinger, J., D. Brady, and J. Geyer. 1974. The heat exchange and transport in the environment, Report 14. Dept of Geography and Environmental Engineering, Johns Hopkins University, Baltimore, MD

[20] Dake J.M.K. and D.R.F. Harlemen. 1969. An analytical and experimental investigation of thermal stratification in lakes and ponds. Hydrodynamics Laboratory Rept No.99, Mass Inst of Technology, Cambridge, MA.

[21] Morrill, J.C., R.C. Bales and M.H. Conklin. 2014. Estimating Stream Temperature from Air Temperature: Implications for Future Water Quality, University of California, School of Engineering, Merced, CA. https://eng.ucmerced.edu/people/rbales/CV/PubsM/98)

[22] Lee K.H. and H.Y. Cho. 2015. Projection of Climate-Induced Future Water Temperature for the

Aquatic Environment. J. Environ. Engr. DOI: 10.1061/(ASCE)EE.1943-7870.0000974
[23] Knauss, J.A. 1997. *Introduction to Physical Oceanography*, 2nd or later editions. Prentice-Hall, upper Saddle River, NJ, 309pp.
[24] Gallegos L.C. 2001. Calculating optical water quality targets to restore and protect submersed aquatic vegetation: overcoming problems in partitioning the diffused attenuation coefficient for photosynthetically active radiation. *Estuaries*, 24(3):381-397
[25] Wang, P., L. Linker, and G. Shenk. 2015. Using geographically isolated loading scenarios to analyze nitrogen and phosphorus exchanges and explore tailored nutrient control strategies for efficient management, *Environ. Model. Assess.* DOI 10.1007/s10666-015-9487-x, pp1-18
[26] Hagy, J.D., Boynton, W.R., Keefe, C.W., Wood, K.V., 2004. Hypoxia in Chesapeake Bay, 1950–2001: long-term changes in relation to nutrient loading and river flow. *Estuaries* 27:634–658.